

STREAMING POTENTIAL MEASURED FOR AN INTACT ROCK SAMPLE AT TEMPERATURES TO 200 °C

Tsuneo Ishido and Nobuo Matsushima

Geological Survey of Japan, AIST
AIST Central 7
Tsukuba, Ibaraki, 305-8567, Japan
e-mail: ishido-t@aist.go.jp

ABSTRACT

Streaming potential was measured in an intact core sample of Inada granite, saturated with aqueous KCl solutions at three different concentrations, at temperatures between 50° and 200°C. We repeated the measurement at each concentration and succeeded in getting fairly reproducible results. The magnitude of the streaming potential coefficient decreases with increasing KCl concentration and increases with increasing temperature. Using a capillary model, we found that the magnitude of the zeta potential and the surface conductance (which dominates the sample conductivity) both increase with increasing temperature. As for the zeta potential, its magnitude is about one fourth of that measured for a crushed sample of Inada granite compared at ~50°C. This small magnitude can be explained by the presence of pores having very small hydraulic radius compared to the thickness of electrical double layer.

INTRODUCTION

Since the 1970's, the SP (self-potential) method has attracted increasing interest in geothermal prospecting and volcanic studies. Among the various mechanisms which can cause SP, the most important appear to be electrokinetic (streaming) potentials arising from underground fluid flow caused by hydrothermal activity and topographic effects (e.g. Zohdy et al., 1973; Zablocki, 1976; Corwin and Hoover, 1979; Ishido, 1989; Ishido et al., 1989; Hashimoto and Tanaka, 1995).

To quantitatively interpret electrokinetic effects deep within the earth, we must estimate *in-situ* values of the cross-coupling coefficients based upon experimental studies of the zeta potential and/or streaming potential coefficient for crustal rock-water systems. Although several experimental studies had been performed (e.g. Ishido and Mizutani, 1981; Ishido et al., 1983; Morgan et al., 1989), experimental measurements describing the effect of temperature upon the cross-coupling coefficients

were sparse until recently, particularly for temperatures above 100°C (Tosha et al., 2003; Reppert and Morgan, 2003). This issue is of crucial importance for quantitative interpretation (such as numerical modeling) of SP observed in geothermal and volcanic areas (e.g. Ishido et al., 1997; Ishido and Pritchett, 1999; Revil et al., 1999b; Ishido, 2004).

EXPRIMENTAL PROCEDURE

Tosha et al. (2003) developed an apparatus to measure the streaming potential of intact rock samples at temperatures up to 200°C (Figure 1). We used this apparatus after adding some modification for the present measurement. A cylindrical rock specimen 30 mm in diameter and 50 mm long was jacketed in a Teflon sleeve (Figure 1b). (We confirmed that no fluid leakage occurs between the upstream and downstream ends by carrying out a test with a dummy glass specimen.) The specimen was electrically isolated from its surroundings by PEEK plates; however, a small electrical leakage was unavoidable through the pore fluid within the upstream and downstream stainless-steel tubes (although it was largely reduced by a Teflon tube inserted within the downstream stainless-steel tube). The electrical impedance Z between the upstream and downstream electrodes is a parallel combination of the sample resistance (R_S) and the impedance leakage path (Z_L), which connects the electrode and the stainless-steel tube through narrow pore fluid path.

To introduce pore fluid, the specimen and the upstream and downstream tubes were evacuated at first. Then, an aqueous solution of known salt concentration (with pH > 6.5 as a result of degasification using Ar gas) was introduced into the tubes and the specimen. One important change from the experimental procedure by Tosha et al. (2003) is that a specimen was left for a few days under the pressure gradient (about 10 bars between the two ends of the specimen) to replace the pore fluid.

After raising the confining pressure to 8 MPa, and increasing the pore pressure to 5 MPa, the

temperature inside the confining vessel was slowly raised to 200°C, which took about 5 hours. Once the furnace was shut down, the temperature gradually began to decline. More than 10 hours were required for the system to cool back to room temperature. At several temperatures between 200°C and room temperature, we measured the streaming potential. First, after closing the downstream valve (valve V_D in Figure 1a), we measured the electrical potential difference between the two electrodes induced by a time-modulated sinusoidal pressure disturbance (amplitude 0.3 MPa, period 30 seconds) imposed upstream. Next, to estimate the sample resistance R_S , we measured the electrical potential difference caused by the pressure change with a known resistance R' connected in parallel with the sample. The magnitude of the impedance Z between the upstream and downstream electrodes was calculated using the formula: $|Z|=|Z'|(\Delta\phi/\Delta P)/(\Delta\phi'/\Delta P)$, where Z' is given by the relation $1/Z' = 1/Z + 1/R'$, and $(\Delta\phi'/\Delta P)$ and $(\Delta\phi/\Delta P)$ are the streaming potential per unit pressure difference with and without the known resistance R' in parallel, respectively.

We used an intact core sample of coarse-grained Inada granite in these experiments, which has a porosity of ~0.9 %. Analyzing the observed attenuation factor and the phase lag between the upstream and downstream pressures (see Figure 2), based upon figure 1 of Fischer and Paterson (1992)

we obtained a rough permeability estimate of $1.5 \times 10^{-18} \text{ m}^2$ for this particular sample.

RESULTS

Streaming Potential Measurement

Figure 2 shows an example of the electrical potential difference recorded between the upstream and downstream electrodes along with corresponding changes in the upstream and downstream pressures. As the plot of the pressure difference (ΔP) and the corresponding potential difference ($\Delta\phi$) across the sample shows, a phase lag was observed between $\Delta\phi$ and ΔP , which is thought to be due to the capacitance in the leakage-current path. In the present study, we simply used the maximum differences in the potential and the pressure, read from graphs like Figure 2, to obtain the streaming potential coefficient ($\Delta\phi/\Delta P$).

Figure 1c shows an equivalent circuit: the drag (streaming) current induced by ΔP flows back as the conduction current through the sample itself (resistance R_S) and through the leakage path, which can be approximated as a series combination of resistance $R_L (=R_{LD}+R_{LU})$ and capacitance $C_L (=C_{LD}^{-1}+C_{LU}^{-1})^{-1}$. So long as the imposed DC-voltage difference across the interface between the aqueous solution and the stainless steel tube is less than ~1 V (which is insufficient for electrolysis reactions),

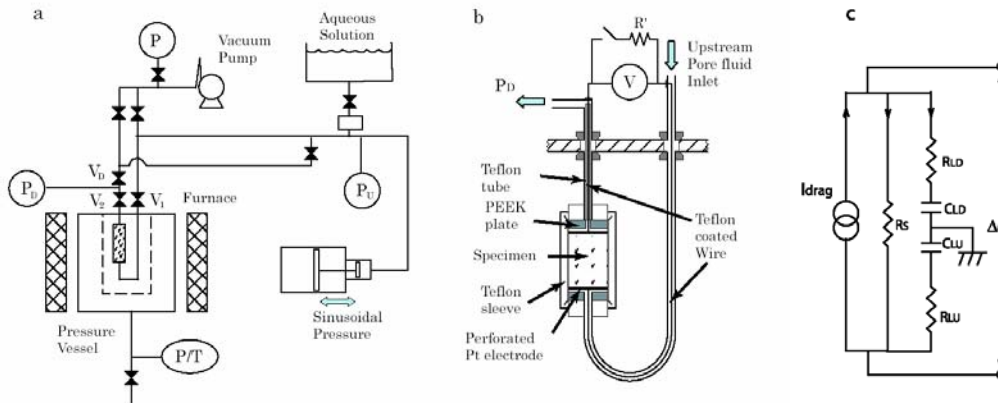


Figure 1 (a) A schematic diagram of apparatus used for streaming potential measurements at high temperatures. During measurements, all valves except V_1 and V_2 are closed. Pressure gauges P_U and P_D measure the upstream and downstream pressures respectively. (b) The rock specimen is electrically isolated by inserting PEEK plates on the outer side of the each perforated-platinum electrode and a Teflon tube inside the downstream stainless-steel tube. A known resistance R' is used for measuring sample resistance. (c) Equivalent circuit. The leakage path is a series combination of resistances R_{LD} and R_{LU} , and capacitances C_{LD} and C_{LU} (where subscripts D and U denote downstream and upstream respectively).

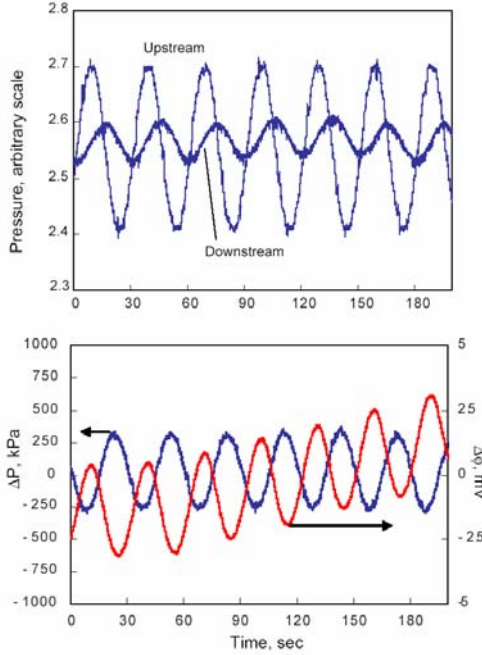


Figure 2. An example of measured data obtained (with 0.1 mol/L solution at 200 °C) while a sinusoidal pressure signal is imposed on the upstream side of the sample.

the current density flowing across the interface will be negligible compared to that expected from the impedance measurement using an LCR meter. The imposed voltage difference is sustained by the electrical double layer at the interface, which acts as a capacitance. The total impedance Z of the circuit shown in Figure 1c is given by the relation;

$$\frac{1}{Z} = \frac{1}{R_S} + \frac{1}{Z_L} \quad \text{where} \quad Z_L = R_L + \frac{1}{i\omega C_L}$$

where the resistance R_L ($\sim R_{LD} \gg R_{LU}$) is estimated as $\sim 10^4 \sigma_F^{-1} \Omega$ (σ_F is the electrical conductivity of the pore fluid in S/m) based on the geometry of the water column within the downstream Teflon tube. The values of R_S and C_L are determined from the observed magnitude and phase of impedance Z . The estimated capacitance is $\sim 2 \times 10^{-5}$, 2×10^{-4} and 3×10^{-4} F on the average for 0.001, 0.01 and 0.1 mol/L KCl solutions, respectively. Resistance R_L is less than R_S for 0.01 and 0.1 mol/L solutions, which tends to shunt current to the leakage path. This is prevented, however, by the presence of interface capacitance.

Figure 3 shows the streaming potential coefficient of our Inada granite sample as a function of temperature for three concentrations of KCl. We used the same rock specimen throughout the present experiments,

and repeated the procedures of replacing pore fluid and the streaming potential measurement at least twice for each concentration of KCl solution until fairly reproducible results were obtained. The magnitudes corrected for the effect of leakage current ($\Delta\phi/\Delta P$) ($R_S/|Z|$) are about 10, 80 and 50 % larger than the observed ones ($\Delta\phi/\Delta P$) for KCl concentrations of 0.001, 0.01 and 0.1 mol/L, respectively.

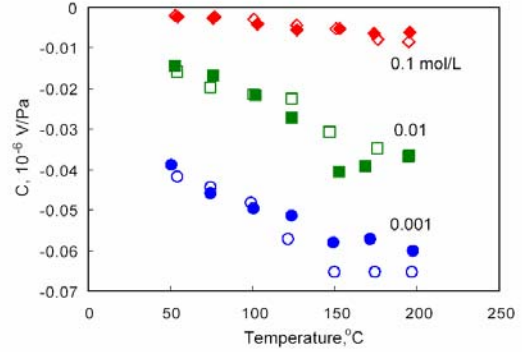


Figure 3. Streaming potential coefficient ($\Delta\phi/\Delta P$) ($R_S/|Z|$) of Inada granite saturated with 0.001 mol/L (circles), 0.01 mol/L (squares) and 0.1 mol/L (triangles) KCl solutions. Open and solid symbols distinguish the data obtained from different runs.

Figure 4 shows the electrical conductivity of the sample (designated L_{ee} hereafter) as a function of temperature for the same three KCl concentrations. The conductivity was calculated as $L_{ee} = l/R_S A$ (where R_S is the sample resistance calculated by the procedure described above, and l and A are the length and cross-sectional area of the specimen respectively).

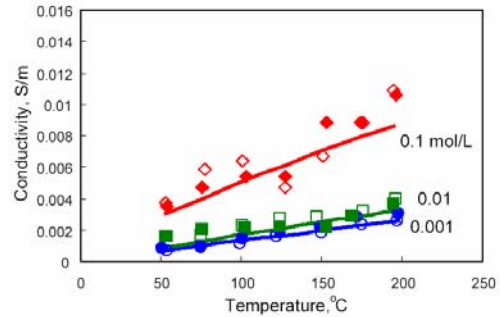


Figure 4. Measured electrical conductivity L_{ee} of Inada granite saturated with 0.001 mol/L (circles), 0.01 mol/L (squares) and 0.1 mol/L (triangles) KCl solutions. Theoretical values based upon equation (2) are also shown.

It should be noted that the conductivity L_{ee} for the 0.001 mol/L solution is nearly the same as that for 0.01 mol/L solution and is within a factor of three or four of that for the 0.1 mol/L solution. This indicates a significant contribution of surface conductance to the total sample conductivity for the more dilute cases.

Zeta Potential Estimation

The electrokinetic coupling coefficient L_{ev} , the electrical conductivity L_{ee} and the streaming potential coefficient C of a porous material are given as follows, according to the capillary model of Ishido and Mizutani, 1981:

$$L_{ev} = -\eta t^{-2} \varepsilon \zeta / \mu \quad (1)$$

$$L_{ee} = \eta t^{-2} (\sigma_F + m^{-1} \Sigma_S) \quad (2)$$

$$C = -L_{ev} / L_{ee} = \varepsilon \zeta / \mu (\sigma_F + m^{-1} \Sigma_S) \quad (3)$$

Here, η and t are the porosity and tortuosity of the porous medium ($\eta t^2 = 1/F$, where F is the formation factor); ε , μ and ζ are the (absolute) dielectric permittivity, dynamic viscosity of the liquid phase and zeta potential, respectively; and σ_F , Σ_S , and m are the electrical conductivity of pore fluid, surface conductance and hydraulic radius of pores and/or cracks.

The theoretical L_{ee} curves shown in Figure 4 are constructed based upon equation (2). The pore fluid (liquid-phase) conductivity (σ_F) is taken to be a function of temperature, pressure and KCl concentration based on the formulation of Olhoeft (1981); the coefficients of the formulation were corrected using data for room temperatures reported in the literature. For surface conductance, we adopt an equation given by Revil et al. (1999b); $\Sigma_S(T) = \Sigma_S(25^\circ\text{C}) \{1 + 0.04(T - 25)\}$ (where T is temperature ($^\circ\text{C}$) and $\Sigma_S(25^\circ\text{C})$ is independent of the salt concentration), and assume $\Sigma_S(25^\circ\text{C}) = 8 \times 10^{-9}$ S, which is the measured value reported by Watillon and de Backer (1970). The theoretical L_{ee} curves reproduce the data fairly well if ηt^2 and m are taken to be $1/0.0012$ and 3×10^{-8} meters respectively, as shown in Figure 4.

Figure 5 shows the ζ potential values obtained by inserting $\varepsilon = \varepsilon(T)$, $\mu = \mu(T)$ and $\sigma_F + m^{-1} \Sigma_S$ (which is used for the theoretical curves in Figure 4) into equation (3). The ζ potential decreases in magnitude with increasing concentration of KCl and increases in magnitude with increasing temperature for all three KCl concentrations. This temperature dependency is similar to the observation for quartz between 25 and 80 $^\circ\text{C}$ (Ishido and Mizutani, 1981). However, the magnitude is quite small (~ 20 mV for 0.001 mol/L

solution at 50 $^\circ\text{C}$) compared to $\zeta \sim -80$ mV obtained in 1981 for a granular Inada granite sample with 0.001 mol/L KNO_3 solution at 45 $^\circ\text{C}$ (Ishido and Mizutani, 1981).

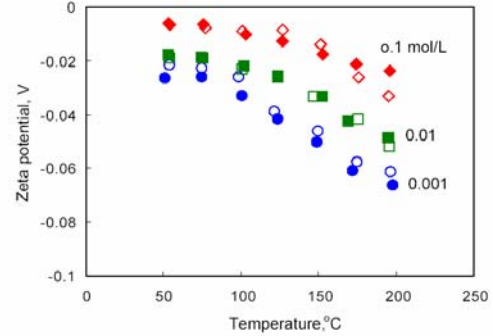


Figure 5. The ζ potential of Inada granite saturated with 0.001 mol/L (circles), 0.01 mol/L (squares) and 0.1 mol/L (triangles) KCl solutions.

DISCUSSION

In the present experiment, the sample cooled from 200 to $\sim 50^\circ\text{C}$ over a 5 hour period, so the temperature during each measurement changed from $T+5$ to $T-5$ $^\circ\text{C}$ in ~ 20 minutes. (Since the decreasing rate was larger than this average at higher temperatures than $\sim 120^\circ\text{C}$, we sometimes turned on the furnace to keep the rate small enough.) This period is too short to achieve equilibrium at room temperature but is sufficient at higher temperatures, since the time required for equilibrium becomes less than ~ 30 minutes above 70 $^\circ\text{C}$ (Ishido and Mizutani, 1981). Thus, most of the data shown in Figure 5 are thought to be close to the equilibrium values.

The present zeta potential obtained for an intact granite sample is small in magnitude compared to the value obtained for crushed granular samples. One of the causes of this discrepancy is thought to be very small hydraulic radius of the sample, which is estimated to be 3×10^{-8} meters by matching the measured and theoretical sample conductivity. This value is in the same order as the thickness of the electrical double layer (=Debye screening length; $\sim 0.9-0.7 \times 10^{-8}$, $0.3-0.2 \times 10^{-8}$ and $0.09-0.07 \times 10^{-8}$ meters for KCl concentrations of 0.001, 0.01 and 0.1 mol/L, respectively). In cases of very small hydraulic radius, the following integral, to which the streaming potential produced by unit pressure difference, i.e. electrokinetic coupling coefficient is proportional (de Groot and Matur, 1962), becomes less than unity.

$$\int_0^\omega (1 - \phi / \zeta) d\Omega / \omega = 1 - G \quad (4)$$

where the integration is over the cross-sectional area (ω) of individual fluid flow path. This integral was evaluated by Burgreen and Nakache (1964) for cases of slit-shaped pores and can be approximated as follows:

$$1 - G = 1 - \tanh(\kappa m) / (\kappa m) \quad (5)$$

where κ : the reciprocal of Debye length and m : hydraulic radius (a half of the slit aperture). In cases that κm is less than 10, G in (5) becomes larger than 0.1. Accordingly, the zeta potential estimated from equation (3) becomes less than $0.9 \times |\zeta|$ in magnitude.

Theoretical zeta potential shown by broken curves in Figure 6 is calculated by using the formula given by Ishido and Mizutani (1981). The pertinent parameters such as adsorption site density ($=1/\text{nm}^2$), the distance between the slipping plane and the solid surface ($=1$ nm and independent of temperature), etc. are adjusted so as to reproduce the measured value for a granular Inada granite ($\zeta \sim -80$ mV with 0.001 mol/L KNO_3 solution at 45°C). The calculated temperature dependency of the zeta potential is about -0.35 mV/ $^\circ\text{C}$ below 100°C for 0.001 mol/L solution, which is close to the observed dependency below 80°C for quartz (Ishido and Mizutani, 1981).

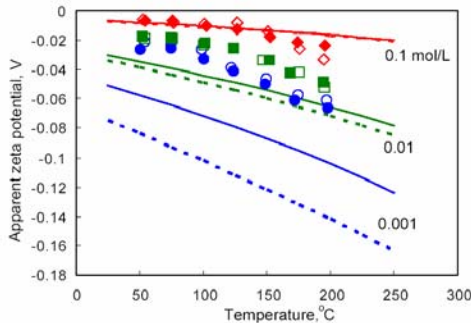


Figure 6. Theoretical zeta potential ζ calculated by Ishido and Mizutani's formula (broken curves) and the apparent zeta potential $\zeta \times [1 - \tanh(\kappa m) / (\kappa m)]$ with $m = 30$ nano-meters (solid curves). Also shown are the data of Figure 5.

The apparent zeta potential: $\zeta \times [1 - \tanh(\kappa m) / (\kappa m)]$ shown by solid curves in Figure 6 is calculated by assuming $m = 3 \times 10^{-8}$ meters. Although quite large reduction in magnitude is seen especially for 0.001 mol/L case, the magnitudes are still larger than the measured values. So, instead of using the hydraulic radius estimated from the conductivity data, we regard it as an adjustable parameter to get better fit with the measured data. The results are shown in

Figure 7. The smaller hydraulic radius assumed here might reflect the substantial population of pores and/or cracks having smaller apertures than the Debye length and large reduction in the factor given by (5).

In Figure 7, also shown are theoretical curves, the zeta potential of which is calculated using the equation $\zeta(T) / \zeta(T_0) = 1 + 0.0171 \times (T - T_0)$ (where T is temperature in $^\circ\text{C}$) given by Revil et al. (1999a, b). $\zeta(T_0 = 25^\circ\text{C})$ is assumed as -54 , -30 and -6 mV for KCl concentrations of 0.001, 0.01 and 0.1 mol/L respectively. Better match is obtained especially for 0.001 and 0.01 mol/L cases.

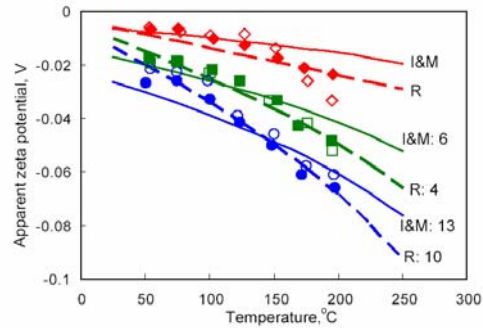


Figure 7. Apparent zeta potential based upon the ζ model by Ishido and Mizutani (solid curves) and that by Revil et al. (broken curves). Numbers indicate the assumed hydraulic radius in nano-meter. Also shown are the data of Figure 5.

CONCLUDING REMARKS

We have changed the experimental procedures from those by Tosha et al. (2003) to allow more complete pore fluid replacement and succeeded in obtaining fairly reproducible values of streaming potential coefficient at high temperatures up to 200°C in the laboratory. Comparing the zeta potentials for 0.001 mol/L solution at $\sim 50^\circ\text{C}$, the magnitude is about one fourth of that measured for a crushed sample of Inada granite (Ishido and Mizutani, 1981). This relatively small magnitude is comparable to that measured for an intact sample of Westerly granite (Reppert and Morgan, 2003) and that of intact granite sample from the Coso field (measured by the present apparatus, and reported by Pritchett et al., 2006). Very small hydraulic radius of pores and/or cracks, which is in the order of the thickness of electrical double layer, is thought to explain more or less the small magnitude of zeta potential estimated from streaming potential measurement of intact crystalline rocks.

The measured streaming potential per unit pressure difference is very small in magnitude, $\sim 1/50$ of

granular samples' values for dilute solutions. This small magnitude is brought about by two effects: the significant contribution of surface conductivity and reduction in the factor given by (5).

The present results show both of the streaming potential coefficient and zeta potential increase in magnitude with increasing temperature. However, the results of Westerly granite (Reppert and Morgan, 2003) and the Coso granite mentioned above do not show such simple temperature dependency. We need further study to clarify the temperature dependency etc. of electrokinetic cross-coupling coefficients of crustal rocks.

REFERENCES

- Corwin, R.F., and D.B. Hoover (1979), The self-potential method in geothermal exploration, *Geophysics*, **44**, 226-245.
- Fischer, G.J., and M.S. Paterson (1992), Measurement of permeability and storage capacity in rocks during deformation at high temperature and pressure, in *Fault Mechanics and Transport Properties of Rocks*, edited by B. Evans and T.-F. Wong, Academic Press, London.
- Hashimoto, T., and Y. Tanaka (1995), A large self-potential anomaly on Unzen Volcano, Shimabara peninsula, Kyushu island, Japan, *Geophys. Res. Lett.*, **22**, 191-194.
- Ishido, T. (1989), Self-potential generation by subsurface water flow through electrokinetic coupling, in *Detection of Subsurface Flow Phenomena, Lecture Notes in Earth Sciences*, vol.27, edited by G.-P. Merkle et al., pp.121-131, Springer-Verlag, New York.
- Ishido, T. (2004), Electrokinetic mechanism for the "W"-shaped self-potential profile on volcanoes, *Geophys. Res. Lett.*, **31**, L15616, doi:10.1029/2004GL020409.
- Ishido, T., T. Kikuchi, N. Matsushima, Y. Yano, S. Nakao, M. Sugihara, T. Tosha, S. Takakura, and Y. Ogawa (1997), Repeated self-potential profiling of Izu-Oshima volcano, Japan, *J. Geomag. Geoelectr.*, **49**, 1267-1278.
- Ishido, T., T. Kikuchi, and M. Sugihara (1989), Mapping thermally driven upflows by the self-potential method, in *Hydrogeological Regimes and Their Subsurface Thermal Effects*, Geophys. Monogr., 47, IUGG Vol. 2, edited by A.E. Beck, G. Garven, and L. Stegena, pp.151-158, AGU.
- Ishido, T., and H. Mizutani (1981), Experimental and theoretical basis of electrokinetic phenomena in rock-water systems and its applications to geophysics, *J. Geophys. Res.*, **86**, 1763-1775, 1981.
- Ishido, T., H. Mizutani, and K. Baba (1983), Streaming potential observations, using geothermal wells and in situ electrokinetic coupling coefficients under high temperature, *Tectonophysics*, **91**, 89-104.
- Ishido, T., and J.W. Pritchett (1999), Numerical simulation of electrokinetic potentials associated with subsurface fluid flow, *J. Geophys. Res.*, **104**, 15,247-15,259.
- Morgan, F.D., E.R. Williams, and T.R. Madden (1989), Streaming potential properties of Westerly granite with applications, *J. Geophys. Res.*, **94**, 12,449-12,461.
- Olhoeft, G.R. (1981), Electrical properties of rocks, in *Physical Properties of Rocks and Minerals*, edited by Y.S. Touloukian, R. Judd, and R.F. Roy, pp.257-329, McGraw-Hill, New York.
- Pritchett, J.W., Garg, S.K., Ishido, T., Matsushima, N., Hase, H. and B.J. Livesay (2006), Evaluating permeability enhancement using electrical techniques (Final technical report for year 2), DOE award number DE-FG36-04GO14291.
- Reppert, P.M. and D. Morgan (2003), Temperature-dependent streaming potentials: 2. Laboratory, *J. Geophys. Res.*, **108**(B11), 2547, doi:10.1029/2002JB001755.
- Revil, A., P.A. Pezard, and P.W.J. Glover (1999a), Streaming potential in porous media 1. theory of the zeta potential, *J. Geophys. Res.*, **104**, 20,021-20,031.
- Revil, A., H. Schwaeger, L.M. Cathles III, and P.D. Manhardt (1999b), Streaming potential in porous media 2. theory and application to geothermal systems, *J. Geophys. Res.*, **104**, 20,033-20,048.
- Watillon, A., and R. de Backer (1970), Potentiel d'écoulement, courant d'écoulement et conductance de surface à l'interface eau-verre, *J. Electroanal. Chem.*, **25**, 181-196.
- Zablocki, C.J. (1976), Mapping thermal anomalies on an active volcano by the self-potential method, Kilauea, Hawaii, in *Proc. 2nd U.N. Symposium on the Development and Use of Geothermal Resources*, vol. 2, 1299-1309, San Francisco.
- Zohdy, A.A.R., L.A. Anderson, and L.J.P. Muffler (1973), Resistivity, self-potential, and induced-polarization surveys of a vapor-dominated geothermal system, *Geophysics*, **38**, 1130-1144.